Applied Catalysis A: General 433–434 (2012) 179–187

Contents lists available at SciVerse ScienceDirect

Applied Catalysis A: General

journal homepage: www.elsevier.com/locate/apcata

Zirconium doped mesoporous silica catalysts for dehydration of glycerol to high added-value products

C. García-Sancho, R. Moreno-Tost*, J. Mérida-Robles, J. Santamaría-González, A. Jiménez-López, P. Maireles-Torres

Departamento de Química Inorgánica, Cristalografía y Mineralogía (Unidad Asociada al ICP-CSIC), Facultad de Ciencias, Universidad de Málaga, Campus de Teatinos s/n., 29071 Málaga, Spain

ARTICLE INFO

Article history:
Received 28 March 2012
Received in revised form 7 May 2012
Accepted 13 May 2012
Available online 22 May 2012

Keywords:
Mesoporous silica
Glycerol
Zirconium oxide
Acid catalysis
Acrolein

ABSTRACT

A series of zirconium doped mesoporous silica, with different Si/Zr molar ratios, has been synthesized and tested in the gas-phase dehydration of glycerol. The surface characterization of these solids by using NH_3-TPD and pyridine adsorption coupled to FTIR spectroscopy has revealed the existence of well dispersed acid sites, mainly of Lewis type, associated to Zr(IV) species deficiently coordinated located on the pore walls of the siliceous framework. These acid catalysts are active in the glycerol dehydration, increasing the conversion with the zirconium content until values higher than 90 mol% for a Si/Zr molar ratio of 4, at 325 °C after 5 h of reaction. However, the catalysts suffer deactivation, which is more important when zirconium oxide is incorporated by impregnation of mesoporous MCM-41 silica. The main reaction products were acrolein, acetaldehyde and acetol. Moreover, the catalysts with a SiZr molar ratio higher than 5 are more selective to acetaldehyde. The acrolein yield was, in all cases, lower than 15 mol% after 24 h of TOS, but a pretreatment under a helium flow saturated with water vapour allows reaching an acrolein yield of 28 mol% and ameliorates the stability of catalysts. The selectivity towards acrolein and hydroxyacetone can be explained by considering the influence of the nature of active sites.

1. Introduction

Acrolein (2-propenal) is the simplest unsaturated aldehyde, with a high synthetic and technical potential due to the conjugation of the carbonyl group with a vinyl group. Acrolein is widely used as intermediate in the production of building materials, herbicides and algaecides, water treatment chemicals, and essential amino acids like methionine used as supplementary in fodder, especially for poultry. At low concentrations, it finds also application for protecting liquid fuels against microorganisms, H_2S scavenger and anti-algae agent.

The current industrial process for acrolein production is by partial catalytic oxidation of propylene. A variety of different catalysts are available for this reaction, the most efficient catalysts are complex mixed-metal oxides that consist largely of Bi, Mo, Fe, Ni, Co, and/or K and either P, B, W, or Sb [1]. The principal side reactions produce acrylic acid, acetaldehyde, acetic acid, carbon monoxide, and carbon dioxide [2,3]. Since propylene is obtained from crude-oil resources, it is desired to utilize a lower cost and renewable raw material for acrolein production, being glycerol a potential candidate. Glycerol is a natural by-product of the manufacture of soap from the hydrolysis of animal fats and vegetable oils. Due to the incessant increment of the worldwide production of biodiesel, the production of glycerol, a by-product of the biodiesel industry, has notably increased causing a drop in its price. In this way, glycerol has been turned into an interesting starting raw material for others chemical products, where the double dehydration of glycerol to acrolein is one of the proposed routes for glycerol valorization. This field of studying has attracted the attention of numerous research groups and in fact, recently, a critical review of acrolein production from glycerol has been released [4].

The dehydration reaction of glycerol yielding acrolein is known since the nineteenth century. Already in 1918, Sabatier et al. reported the decomposition of glycerol to different products, including acrolein, in the presence of alumina catalysts [5]. Because of crude glycerine is found diluted in water, the catalysts must be active and resistant to the presence of water avoiding a separation step of the glycerol from the water and therefore reducing the price of production of acrolein. Various solid acid catalysts have been tested in the dehydration of glycerol, including zeolites [6–10], supported heteropolyacids [11–14] and phosphoric acid impregnated activated carbon [15] or Al_2O_3 and TiO_2 [16], niobium oxide [17,18] and WO_3/ZrO_2 catalysts [19,20] in a gas phase reaction. Several studies have demonstrated that the catalytic activity depends on the textural, mainly the pore size, and acid properties of the solid catalysts, as recently reviewed by Pathak et al. [21]. Thus,

* Corresponding author. Tel.: +34 952132021; fax: +34 952131870.
E-mail address: rmtost@uma.es (R. Moreno-Tost).

0926-860X/$ – see front matter © 2012 Elsevier B.V. All rights reserved.
http://dx.doi.org/10.1016/j.apcata.2012.05.015

Tsukuda et al. [13] claimed that catalysts with small pores showed low catalytic activity, as long as catalysts with a mesopores ranged between 6 and 10 nm showed a high glycerol conversion and high selectivity towards acrolein. It seems to be accepted that Brönsted acid sites of weak-moderate strength catalyse acrolein production [9,10,17,19], whereas Lewis acid sites and the presence of basic sites increased the selectivity of hydroxyacetone (acetol) [22–24].

However, the main drawback of most tested acid catalysts concerns the deactivation by coke formation on the catalyst surface [14,16,17], due to the acid strength and the pore network, although in some cases the catalytic activity can be recovered by calcining the catalyst at temperatures above 500 °C in flowing air [18]. Corma et al. [25] reported that glycerol in water can be converted into acrolein, olefins, and acetaldehyde by using zeolites in a continuous fluidized-bed reactor, where continuous regeneration can be performed, if needed. The stability against deactivation has been also reached by doping caesium 12-tungstophosphate salt with platinum group metals, together with co-feeding hydrogen [26]. Katryniok et al. [4] showed a long-time performance of a catalyst based on silicotungstic acid supported on SBA-15 grafted with ZrO_2. This effect was interpreted in terms of modification of the interaction between the support and the heteropolyacid which results in a lower Brönsted acidity. Lauriol-Garbay et al. [27] have synthesized a catalyst based on a mixed Zr–Nb oxide which exhibits a promising stability (82% glycerol conversion after 177 h on stream). The key of the stability of these catalysts is the coverage of Lewis acid sites by polymeric Nb oxide species which were the unselective coke initiator sites. Another technical improvement in the dehydration of glycerol was proposed by Yan et al. [15], by using a low-pressure packed bed reactor to favour the evaporation of glycerol and remove reaction mixture from dew-points. Thus, the formation of liquids on the catalyst surface was not favoured and, therefore, the coke formation is decreased.

The aim of this research is to test a family of zirconium doped mesoporous silica catalysts in the dehydration of glycerol to add value chemicals. These catalysts possess analogous textural properties but different acidities depending on the degree of zirconium doping, which effect on their catalytic activity, selectivity and stability has been evaluated.

2. Experimental

2.1. Catalysts synthesis

A series of zirconium doped mesoporous MCM-41 silica, with different Si/Zr molar ratios, has been synthesized by following the method proposed by Jones et al. and reported in previous papers [28,29]. Briefly, it was prepared by adding appropriate amounts of tetraethoxysilane and zirconium *n*-propoxide to an ethanol–propanol solution, which was stirred at room temperature for 15 min, and then added to an aqueous solution of hexadecyltrimethylammonium bromide (25 wt.%), previously stirred at 80 °C for 30 min. The surfactant/(SiO_2 + ZrO_2) ratio was 0.5. The pH was adjusted to 10 by addition of an aqueous solution of tetramethylammonium hydroxide (25 wt.%), and the resulting gel was stirred at room temperature for 4 days. Solid product was recovered by centrifugation, washed several times with ethanol, dried at 70 °C, and then calcined in air at 550 °C for 6 h (1 °C min^{-1} heating rate) in order to remove the surfactant molecules. Three different Si/Zr molar ratios (4, 5 and 10) were used and the catalysts were labelled as SiZr*x*, where *x* indicates the Si/Zr molar ratio.

For comparison reasons, a catalyst with the same weight percentage of ZrO_2 as the SiZr5 catalyst (30 wt.%) has been prepared by wet impregnation of a pure MCM-41 silica. Then, the catalyst was dried and calcined in air under the same conditions as SiZr*x* catalysts. This catalyst was labelled as Si–30Zr. On the other hand, the SiZr5 catalyst has been treated in a flow of He saturated with steam during 4 h at 315 °C, and the resulting solid was labelled as SiZr5-315.

2.2. Catalyst characterization

Powder XRD measurements were performed on a Siemens D5000 automated diffractometer, over a 2θ range with Bragg–Brentano geometry using the Cu Kα radiation and a graphite monochromator. Thermogravimetric and differential thermal analyses (TG-DTA) were performed on a Pyris-Diamond PerkinElmer apparatus. The temperature was varied from room temperature up to 1000 °C, at a heating rate of 10 °C min^{-1} with a flux of air of 100 mL min^{-1}, using a mass around 15 mg.

X-ray photoelectron spectroscopy (XPS) studies were performed with a Physical Electronics PHI 5700 spectrometer equipped with a hemispherical electron analyzer (model 80-365B) and a Mg Kα (1253.6 eV) X-ray source. High-resolution spectra were recorded at 45° take-off-angle by a concentric hemispherical analyzer operating in the constant pass energy mode at 29.35 eV, using a 720 mm diameter analysis area. Charge referencing was done against adventitious carbon (C 1s at 284.8 eV). The pressure in the analysis chamber was kept lower than 5×10^{-6} Pa. PHI ACCESS ESCA-V6.0 F software package was used for data acquisition and analysis. A Shirley-type background was subtracted from the signals. Recorded spectra were always fitted using Gauss–Lorentz curves in order to determine more accurately the binding energy of the different element core levels.

N_2 adsorption–desorption isotherms at −196 °C were obtained using an ASAP 2020 model of gas adsorption analyzer from Micromeritics, Inc. Prior to N_2 adsorption, the sample were evacuated at 200 °C (heating rate 10 °C min^{-1}) for 18 h. Pore size distributions and pore volume were calculated with the BJH method.

Evolved gas analysis at programmed temperature by mass spectrometry (EGA-MS) was carried out to the spent catalysts. The evolved H_2O and CO_2, arising from the combustion of the carbonaceous deposits, were monitored by recording the m/z = 18 and 44 signals, respectively. 80 mg of the sample was loaded in a quartz microreactor and 50 mL (STP) min^{-1} of O_2 (5 vol.% O_2 in He) were passed through while the sample was heated at 10 °C min^{-1}. A quadrupole mass spectrometer, model BALZERS Prisma QMS 200 controlled by BALTZER QuadstarTM 422 software, was connected on-line to the reactor outlet for the analysis of gases generated.

FTIR spectra of adsorbed pyridine were recorded on a Shimadzu 8300 FTIR spectrometer at a resolution of 4 cm^{-1}. Each spectrum was average over 128 scans. Self-supporting wafers of samples with a weight/surface ratio of about 12 mg cm^{-2} were placed in a vacuum cell with greaseless stopcocks and CaF_2 windows. Solids were evacuated at 350 °C and 10^{-4} Torr overnight, exposed to pyridine vapours for 15 min at room temperature, and then degassed at different temperatures. The net FTIR spectra of adsorbed pyridine were obtained after subtracting the background spectrum of the solid.

2.3. Catalytic reaction

The dehydration of glycerol was performed, at atmospheric pressure, in a fixed-bed continuous-flow stainless steel reactor (9.1 mm in diameter, and 230 mm in length), operated in the down-flow mode. The reaction temperature was measured with an interior placed thermocouple in direct contact with the catalyst bed. For the activity tests, 0.3 g of catalyst (particle size 0.85–1.00 mm), diluted with SiC to 3 cm^3 volume, was used. Catalysts were pre-treated in situ at atmospheric pressure under a

Table 1
Textural and acid characteristics of SiZr*x* catalysts.

Catalyst	S_{BET} (m^2/g)	V_p (cm^3/g)	d_p (nm)	TPD-NH_3 (μmol/(g cat))	TPD-NH_3 (μmol/m^2)
SiZr4	626	0.627	3.1	480	0.77
SiZr5	652	0.671	3.3	326	0.50
SiZr10	685	0.597	2.7	262	0.38
MCM-Si	1000	0.824	2.5	n.d.	n.d.
Si–30Zr	562	0.378	1.8	11	0.02

n.d., no detectable.

nitrogen flow of 30 mL min^{-1} at 325 °C for 30 min. The glycerol solution (10 wt.% in water) was supplied by means of a Gilson 307SC piston pump (model 10SC) at 0.05 mL min^{-1} feed rate in a N_2 flow (30 mL min^{-1}). The evolution of catalytic tests was studied by collecting liquid samples after 5 and 24 h in a vial cooled in an isopropanol–liquid N_2 trap. These vials were sealed for posterior analysis by gas chromatography. The reaction products were analysed by means of gas chromatograph (Shimadzu GC-14B), equipped with a flame ionization detector and a capillary column (TRB-14).

The glycerol conversion (mol%) and the selectivity to the identified and calibrated products have been calculated as follows:

$$C_{Gly} = \frac{n_{Gly,in} - n_{Gly,out}}{n_{Gly,in}} \times 100 \quad \text{and}$$

$$S_l = \frac{n_i}{n_{Gly,in} - n_{Gly,out}} \times \frac{z_i}{z_{Gly}} \times 100$$

where n_{in} and n_{out} represent the mol of glycerol at the inlet and outlet of the reactor. n_i are the molar concentration of the product i at the outlet of the reactor and z_i and z_{Gly} are the number of atoms of carbon of the product i and glycerol. The carbon balance (mol%) was calculated by summing up the unreacted glycerol and the total quantities of detected and calibrated products.

3. Results and discussion

3.1. Catalysts characterization

In this paper, a series of zirconium-doped mesoporous silica, previously used as support of different active phases [30,31], has been tested in the gas-phase dehydration of glycerol. The mesoporous character of these solids has been confirmed by the analysis of the adsorption-desorption isotherms of N_2 at −196 °C (Fig. 1a). The isotherms of all synthesized materials are of type IV according to the IUPAC classification. All of them exhibit the sharp capillary condensation step at relative pressures of 0.3–0.4. Moreover, it is observed an unimodal pore size distribution (Fig. 1b), typical of mesoporous materials. Their high specific surface areas, pore volumes and pore sizes reveal the mesoporous nature of this family of zirconium doped silica (Table 1). The hexagonal structure of mesoporous materials (Fig. 2) has been proven by means of the X-ray diffraction technique because, after calcination at 550 °C, all the materials exhibit in their XRD patterns the intense and broad low-angle diffraction peak assigned to the (1 0 0) diffraction planes, except the SiZr4 catalyst which points out its lack of long-range order. The absence of other well-defined diffraction peaks in the region $2\theta = 3–8°$ can be justified by the low temperature used in the synthesis of these mesoporous materials, differently from those reported in most of papers, which are synthesized under hydrothermal conditions at higher temperatures. Moreover, XRD patterns in the high-angle region did not evidence the characteristic reflections of crystalline ZrO_2 phases, thus pointing to the existence of amorphous or ZrO_2 species of small size on the silica walls.

It has been reported that the catalyst acidity is one of the key factors affecting the catalytic performance in the glycerol dehydration to yield acrolein [32–34]. The surface concentration of acid sites has been evaluated by means of TPD-NH_3. It is generally accepted that the acid strength depends on the ammonia desorption temperature: weak (100–200 °C), medium (200–400 °C) and strong (>400 °C) [35]. The absence of distinguishable maxima on the TPD-NH_3 curves (Fig. 3) makes difficult their deconvolution. Therefore, the acidity of catalysts has been calculated by integrating the curves in the range between 100 and 550 °C (Table 1). Moreover, the intrinsic acidity of the catalysts or density of acid sites (μmol of NH_3/m^2) is reported in Table 1. These curves are broad and the complete ammonia desorption is not achieved even at 550 °C, evidencing a heterogeneous distribution of acid strengths, although the weak-medium acid sites are predominant since the majority of ammonia is desorbed between 100 and 400 °C. Thus, SiZr*x* catalysts

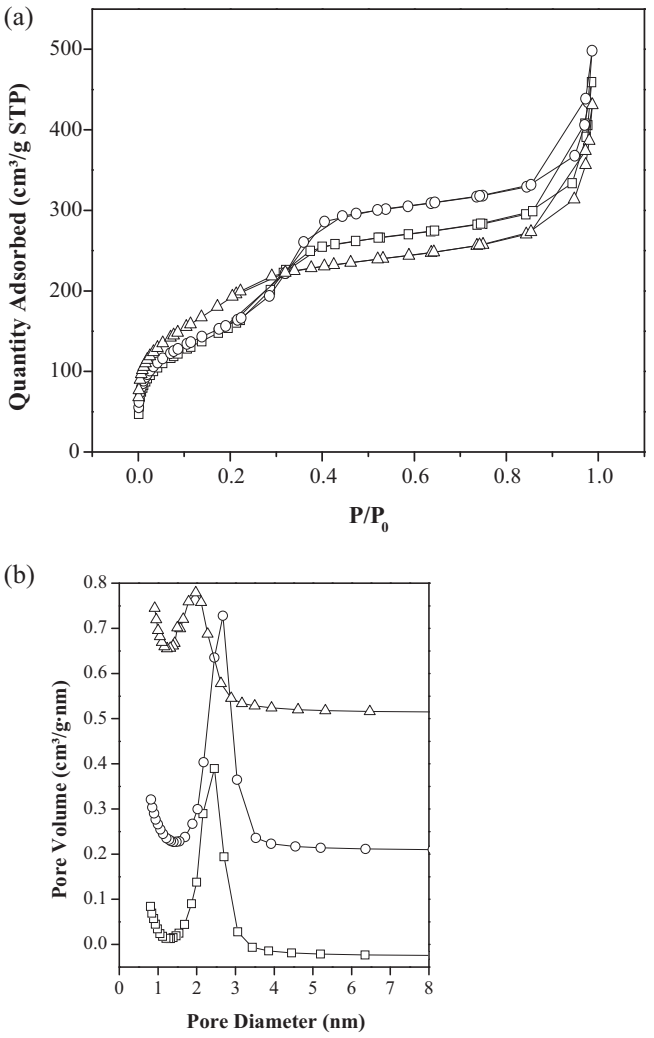

Fig. 1. (a) Nitrogen adsorption isotherms of SiZr*x* catalysts: SiZr4 (□), SiZr5 (○) and SiZr10 (△); and (b) pore size distributions of SiZr*x* catalysts: SiZr4 (□), SiZr5 (○) and SiZr10 (△).

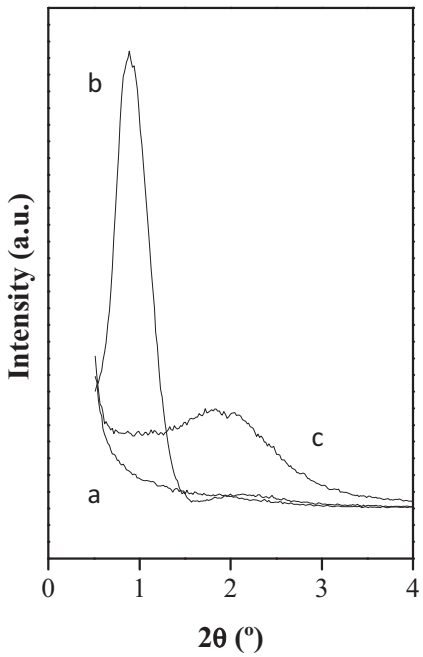

Fig. 2. Powder XRD patterns at low angle of SiZr*x* catalysts: SiZr4 (a), SiZr5 (b) and SiZr10 (c).

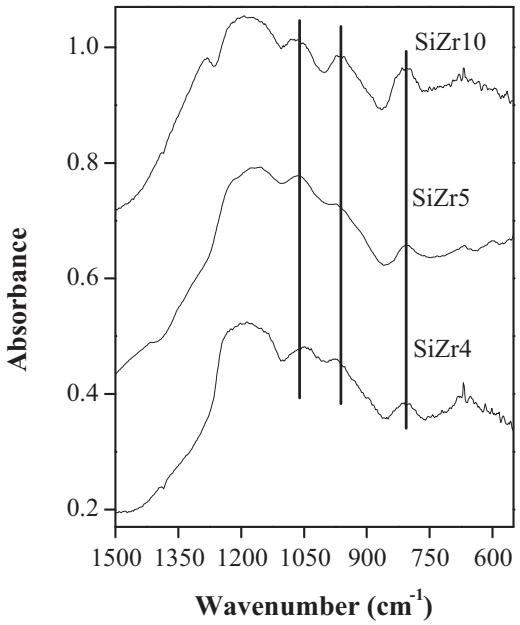

Fig. 4. FTIR analysis of the SiZr*x* in the range 600–1500 cm^{-1}.

display a total acidity higher than pure mesoporous silica [36] and it is noticeable the increase in the acidity with the amount of Zr incorporated to the framework, being the SiZr4 catalyst the most acidic among the SiZr*x* catalysts (Table 1). In general, the intrinsic acidity of SiZr*x* catalysts is lower than those reported for zeolites [34], SAPO catalysts [16], Me–Al_2O_3–PO_4 [37] and Zr-TUD-1 samples [38] but, on the other hand, the acidity of SiZr*x* is higher than that exhibited by a hexagonal ordered mesoporous silica grafted with 20 wt.% ZrO_2 [4] or Al incorporated in the framework [10], or quite similar to a montmorillonite pillared with ZrO_2 [39]. The acid sites are mainly due to the presence of Zr into the mesoporous network where superficial Zr(IV) species with low coordination exist. The presence of Zr in the framework of the siliceous mesoporous material has been proven by means of FTIR of the SiZr*x* catalysts (Fig. 4). These catalysts show some characteristics features, such as the asymmetric stretching vibration of Si—O—Si bonds found at

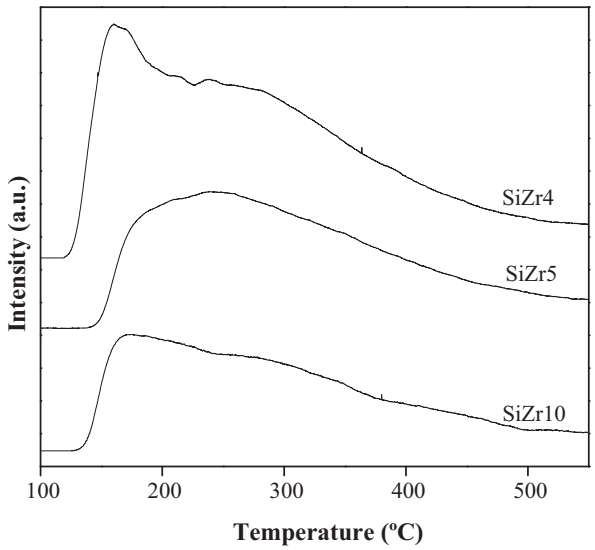

Fig. 3. TPD-NH_3 curves of SiZr*x* catalysts.

1050–1070 cm^{-1}, which intensity gradually is reduced as the Zr content increases. The red shift of this band with the increase of zirconium content is a demonstration of the replacement of Si atoms in the framework by Zr atoms [40]. The band at 808 cm^{-1} is associated to the Si—O—Si symmetric stretching [41] and finally, the band at 970 cm^{-1} is ascribed to the Si—(OH) stretching of terminal silanols [38,29].

One commonly used method to characterize the nature of the acid sites (Brönsted or Lewis) is the study of the shift of the IR and Raman vibration bands of basic probe molecules when adsorbed on the catalyst surface [42]. In this sense, the adsorption of pyridine is widely used as probe molecule [10,22,43] since different adsorbed pyridine species can be observed: pyridine bonded by hydrogen interaction on weakly acidic OH groups, pyridine on deficiently coordinated centres (Lewis sites) and protonated pyridine on Brönsted sites. In this way, the acid sites have been characterized by adsorption of pyridine after outgassing at different temperatures (Fig. 5 and Table 2). The concentration of both types of acid sites has been estimated from the integrated absorption at 1550 and 1450 cm^{-1} using the extinction coefficients $E_B = 0.73$ cm μmol^{-1} and $E_L = 1.11$ cm μmol^{-1} for Brönsted and Lewis sites, respectively. The IR spectra of the SiZr5 catalyst, after pyridine adsorption and outgassing at 100 and 200 °C, are shown in Fig. 5. The SiZr10 and SiZr4 catalysts exhibit the same bands after contacting with pyridine vapours. The SiZr5 catalyst displays bands at 1446 and 1596 cm^{-1}, assigned to pyridine adsorbed on weak Lewis acid sites or to weakly hydrogen-bonded pyridine [22,44,45]. The band at 1577 cm^{-1} can be also ascribed to pyridine adsorbed on weak Lewis acid sites [46]. These bands are almost vanished after outgassing at 100 °C, thus revealing the existence weak Lewis acid sites. The bands at 1637 and 1544 cm^{-1} can be assigned to pyridinium ring vibrations, due to the proton transfer from Brönsted acid sites to pyridine [34,46]. After outgassing at 100 and 200 °C, the bands associated to Brönsted sites are still present on the surface of catalysts. Finally, outgassing at temperatures higher than 200 °C provokes the disappearance of bands associated to pyridine bonded to both Brönsted and Lewis centres. It is well-known that pure MCM-41 silica and ZrO_2 are Lewis solids without Brönsted acid sites [43,44]; therefore, the Brönsted acid sites in the silica MCM-41 network detected by the adsorption of pyridine coupled with FTIR are caused by the

Table 2
Concentration of Brönsted and Lewis acid sites of SiZr*x* catalysts, after evacuation at different temperatures.

Catalyst	Evacuation temperature (°C)	Brönsted[a] sites (μmol/g)	Lewis[a] sites (μmol/g)	$I_B/(I_B+I_L)$
SiZr4	100	68.5	51.9	0.57
	200	8.8	7.4	0.54
SiZr5	100	36.3	9.2	0.80
	200	35.9	0	1.0
SiZr10	100	107.1	88.4	0.54
	200	32	34.9	0.50
SiZr5-315	100	107.8	50.3	0.68
	200	105.7	11.8	0.90

[a] Concentration of acid sites calculated from the extinction coefficients calculated by Datka et al., J. Catal. 135 (1992) 186–199.

Table 3
Surface characterization of SiZr*x* catalysts determined by XPS analysis.

Catalyst	O1s (eV)	$Zr3d_{5/2}$ (eV)	Atomic ratio	
			Si/Zr	O/(Si + Zr)
SiZr4	531.1 (12.5%) 533.2 (87.5%)	182.7	9.8	2.1
SiZr5	531.3 (8.1%) 533.2 (91.9%)	182.8	13.2	2.2
SiZr10	531.6 (4.8%) 533.2 (95.2%)	182.8	46.7	2.2

presence of atoms of Zr replaced the Si ones [45]. The origin of these Brönsted acid sites has been related to changes in electron density on Si, due to charge imbalance or difference of electronegativity, resulting from introduction of Zr atom in the vicinity of the Si—OH, weakens the SiO—H bond and generates Brönsted acidity [47].

The superficial enrichment of Zr is corroborated by XPS, since the surface Si/Zr atomic ratio increases with the Si/Zr molar ratio used in the synthesis gel (Table 3). The XPS analysis in the region of O1s signal becomes more asymmetric as the Zr content is higher, indicating the existence of two different oxygen environments. This O1s band can be deconvoluted into two components: Si—O—Zr (at 531.1 eV) and Si—O—Si (at 533.2 eV), the former increasing their intensity with the Zr content at expense of the later, indicating the replacement of Si by Zr atoms. The presence of segregate ZrO_2 could be ruled out by the lack of the O 1s band at 529 eV [48] and furthermore, the binding energies of Zr $3d_{5/2}$ (182.7 eV) are higher than that of ZrO_2 (182.2 eV) supporting the incorporation of the heteroatom in the siliceous framework. The higher binding energy of the Zr $3d_{5/2}$ band of SiZr*x* catalysts implies a higher ionic character of the bonding Zr—O [45,49] and therefore involving a higher positive charge over Zr which leads to a stronger Lewis acidity in these materials.

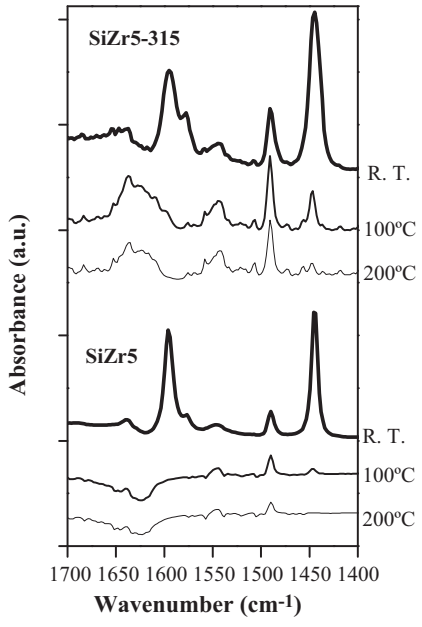

Fig. 5. FTIR analysis of pyridine adsorption on SiZr5 and SiZr5-315 catalysts, after outgassing at 100 and 200 °C.

3.2. Catalytic performance

In the dehydration of glycerol to yield acrolein, ZrO_2 has been used as support of WO_3 [19], where its seems to ameliorate the long-term stability of catalysts [4,12]. Moreover, Chai et al. [32] have reported an acrolein yield of 7 mol% at 315 °C, after 9–10 h of time-on-stream and glycerol GHSV = 80 h^{-1} when ZrO_2 was employed.

Preliminary experiments were carried out to rule out the contribution to the overall glycerol conversion of silicon carbide, which has been used as diluents of the catalysts. The results show that SiC is inert in the whole range of tested temperatures (275–350 °C), hence the glycerol conversion observed must be associated to the catalysed process. Moreover, at these reaction temperatures, a thermal homogenous glycerol conversion has not been observed.

The analysis of the liquid phase, after 5 and 24 h of time on stream (TOS) at 325 °C, reveals the formation of acrolein, acetaldehyde and hydroxyacetone as main products, as well as acetone, ethanol, methanol, allyl alcohol and propanaldehyde were detected as minor components. These minor components along others no analysed have been included in the column labelled as *Others* (Table 4). The unidentified products can be possibly formed by secondary reactions among products or between products and glycerol, together with gaseous species such as CO and CO_2. In spite of those unidentified products, the carbon balance was usually above 90 mol%, except for the SiZr4 catalyst [37,43,50]. Full conversion of glycerol is not accomplished with none of the tested catalysts within the first 5 h of reaction, although SiZr4 and SiZr5 catalysts lead to glycerol conversion close to 90 mol%, whereas the glycerol conversion found for the SiZr10 catalyst is lower (73 mol%), which reveals that glycerol conversion increases with the total acidity of catalysts [16]. However, after 24 h of TOS, all the tested catalysts exhibit some degree of deactivation, being less pronounced in the case of the SiZr4 catalyst which maintains a glycerol conversion of 73 mol%. The SiZr4 catalyst is the most active and stable, but it is not the most selective to acrolein (Table 4) since its selectivity to acrolein is 14 mol% after 24 h of TOS, being the SiZr5 catalyst the most selective to acrolein with a value of 31 mol%. Along with acrolein, acetaldehyde is the major reaction product, which has been proposed as a decomposition product of 3-hydroxypropanaldehyde [13,16,51]. On the other hand, the acetol (hydroxyacetone) is also detected as dehydration product of glycerol (Table 4). In fact, in the case of the SiZr10 catalyst, the hydroxyacetone is the major constituent among the reaction products, reaching up to 24 mol% of selectivity after 24 h of TOS.

Table 4
Glycerol conversion and product selectivity over SiZr*x* catalysts, at 325 °C.

Catalyst	TOS (h)	Conversion (%)	Product selectivity (%)					Acrolein yield (%)	C balance (%)
			Acrolein	Acetaldehyde	Acetol	Allyl alcohol	Others		
SiZr4	5	92	15	19	13	3	50	13	57
	24	73	14	22	17	2.7	44	10	68
SiZr5	5	89	26	29	21	0	24	23	79
	24	47	31	37	14	0	18	15	91
SiZr5-315	5	97	40	33	13	0	15	38	86
	24	80	35	35	23	1.7	5	28	96
SiZr10	5	73	24	28	30	8.3	10	19	93
	24	44	19	22	24	5.2	30	11	87
Si–30Zr	5	51	81	9	11	0	0	41	100
	24	12	0	17	46	0	37	0	99

Experimental conditions: weight of catalyst = 0.3 g diluted with SiC to 3 cm^3 volume. Feed composition: 10 wt.% glycerol in water; liquid flow = 0.05 mL min^{-1}; N_2 flow = 30 mL min^{-1}; T = 325 °C.

The acrolein selectivity after 24 h TOS decreased in the order: SiZr5 > SiZr10 > SiZr4. This selectivity trend is also observed for the acetaldehyde which is the main reaction product obtained at 325 °C. However, the selectivity to hydroxyacetone reached a minimum for SiZr5 catalyst.

These SiZr*x* catalysts show a reaction product distribution quite different to that reported in bibliography. Thus, Chai et al. [11,12,32] reported that bulk ZrO_2 showed acrolein selectivity lower than 10 mol% and hydroxyacetone appeared as the main product. Tao et al. [52] reported that mixed silica zirconia showed acrolein selectivity of 15 mol% for a 20 mol% of ZrO_2 and acrolein selectivity of 21 mol% if the molar percentage of ZrO_2 was increased up to 75%, after 10 h of TOS. In this case, the hydroxyacetone was also the main by-product and acetaldehyde selectivity was as low as 5 mol%. Stosic et al. [24] reported a commercial zirconia with a glycerol conversion of 59% after 90 min TOS and an acrolein selectivity of 5 mol% and hydroxyacetone selectivity of 25 mol%. As it is known, zirconia is a typical Lewis acid solid, so in the dehydration reaction of glycerol, the selectivity is addressed to the formation of hydroxyacetone instead of acrolein, even though a significant conversion of glycerol is displayed. Finally, it is noticeable to mention that the SiZr*x* catalysts show a better catalytic performance than those reported in bibliography based on bulk or mixed oxides with ZrO_2 [11,24,52,54].

In general, the mechanisms proposed to explain the large variety of products coming from this reaction distinguish two main pathways for glycerol activation. On the one hand, on Lewis acid sites, the terminal OH of glycerol is activated leading to the formation of hydroxyacetone, but, on the other hand, on Brönsted acid sites, the secondary OH protonation occurs evolving towards the acrolein formation [4,9,17,25,32,43]. The results of pyridine adsorption have shown the presence of both Brönsted and Lewis acid sites on the SiZr*x* catalysts and therefore, the two reaction paths cannot be ruled out. Thus, the formation of acrolein indicates a mechanism based on protonation of the secondary alcohol of glycerol to form the unstable 3-hydroxypropanaldehyde, intermediate which suffers dehydration to form acrolein. The by-product hydroxyacetone is formed after activation of glycerol on the Lewis acid sites present on the surface of the catalysts. Kim et al. [55] have reported a correlation between the hydroxyacetone yield and the concentration of Lewis acid sites. The hydroxyacetone formation has been also described by Auneau et al. [56] in the hydrogenolysis of glycerol to 1,2-propanediol by means of a dehydration mechanism on the Rh(1 1 1) surface. The formation of acetaldehyde could happen from the unstable 3-hydroxypropanal, via a retro-aldol reaction [13,32] or from hydroxyacetone as Suprun et al. [16] or Lauriol-Garbey et al. [50] have reported. Corma et al. [25] also reported other way for the acetaldehyde formation from an unstable dione, which decomposes rapidly into CO and acetaldehyde. According to the pyridine tests, the selectivity pattern could be explained by taking into account the nature of the acid sites. Thus, the SiZr5 catalyst is the most selective to acrolein due to its higher B/(L + B) acid sites ratio (Table 2) among the tested catalysts, and the SiZr10 catalyst is the most selective to hydroxyacetone since it possesses the higher concentration of Lewis acid sites.

Several authors [22,26] have reported that Brönsted sites can be generated on the catalyst surface from Lewis sites if water is present, with a concomitant increasing of the selectivity to acrolein. In order to transform Lewis acid sites into Brönsted ones, the SiZr5 catalyst was pre-treated in a helium flow saturated with steam water at 315 °C for 4 h. This pretreatment of the SiZr5 catalyst leads to an important increase of the concentration and strength of Brönsted acid sites in detrimental of the Lewis acid centres, as evidenced the FTIR spectrum after outgassing at 200 °C (Table 2 and Fig. 5). This shift in the distribution of acid sites ameliorates the stability of catalysts against deactivation, since the glycerol conversion hardly decreases after 24 h of TOS (Table 4) and the acrolein yield is increased until 28 mol%. Moreover, the selectivity to acetol is lower after 5 h of TOS, revealing that a fraction of Lewis acid sites are converted in Brönsted sites after the steaming treatment, although after 24 h the selectivity to acetol is higher than that observed for SiZr5 catalyst.

The evaluation of the effect of reaction temperature on the dehydration of glycerol was examined over the SiZr5 catalyst, after 5 h of TOS (Fig. 6). As it was expected, the glycerol conversion remarkably increased with the reaction temperature from 275

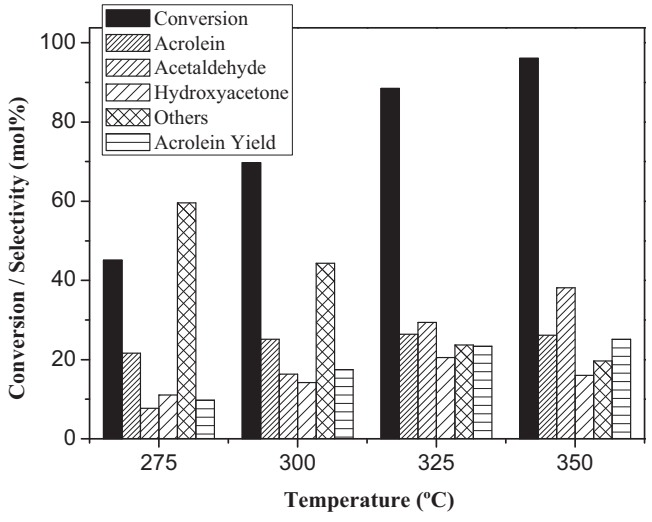

Fig. 6. Conversion and selectivity of glycerol dehydration over SiZr5 as a function of the reaction temperature. Experimental conditions: weight of catalyst = 0.3 g diluted with SiC to 3 cm^3 volume. Feed composition: 10 wt.% glycerol in water; Liquid flow = 0.05 mL min^{-1}; N_2 flow = 30 mL min^{-1}.

Table 5
Characterization of spent SiZr*x* catalysts.

Catalyst (TOS = 24 h)	S_{BET} (m^2/g)	V_p (cm^3/g)	d_p (nm)	Weigth loss[a] (%)	CHN analysis		
					C (mol%)	H (mol%)	H/C
SiZr4	389	0.614	5.3	16.3	0.83	1.32	1.58
SiZr5	251	0.279	3.5	11.4	0.64	1.31	2.05
SiZr10	194	0.438	6.4	13.4	0.90	1.71	1.90

[a] From TG results.

to 350 °C. Thus, Ulgen et al. [20] stated that temperatures lower than 280 °C favoured the intermolecular dehydration, yielding glycerol oligomers instead the intramolecular dehydration leading to acrolein. These authors claimed that these oligomers are responsible of the decrease of the acrolein selectivity at low temperatures. The acrolein yield increases slightly with the reaction temperatures, reaching a value of 26 mol% at 325 °C. It is noteworthy the important decrease in the selectivity to *Others* by increasing the reaction temperature. This catalytic behaviour had been already observed by Corma et al. [25], who pointed an increase of coke deposited on the catalysts when the reaction temperature decreased from 350 until 290 °C, while observing a lower production of by-products whereas the acrolein production remained almost unchanged throughout the tested temperature range. On the other hand, the acetaldehyde selectivity increased with the temperature, reaching the highest value at 350 °C, similarly to that reported by Kim et al. [34] for H-zeolites. Haider et al. [53] consider that at temperatures higher than 290 °C the formation of acetaldehyde could be preferential via a retro aldol fragmentation of 3-hydroxypropanal. At the same time, the selectivity to acetaldehyde is increased at 350 °C, the hydroxyacetone selectivity is decreased and the acrolein selectivity is maintained. Lauriol-Garbey et al. [50] observed the same behaviour, and they pointed out that hydroxyacetone could be converted to acetaldehyde and acetone over acidic sites.At the beginning of this section, it was mentioned that a key characteristic of zirconia is to ameliorate the long-term stability of catalysts in the dehydration of glycerol, but up to date it has not been tested as an active phase itself, i.e. zirconia have been only used as support or stabilizer of an active phase. Furthermore, we have proved that SiZr*x* catalysts show better catalytic performance that those tested in bibliography based only on ZrO_2. On the other hand, since the discovery of M41S solids by Mobil researchers, their excellent textural properties have encouraged their use to disperse catalytically active phases. Therefore, we have prepared a catalyst by dispersing ZrO_2 in a pure MCM-41 silica and compared its catalytic activity with that of the SiZr5 catalyst. Thus, mesoporous MCM-41 silica has been impregnated with 30 wt.% ZrO_2, an analogous Zr content to that of the SiZr5 catalyst, and tested in the dehydration of glycerol. The main textural properties of this catalyst are collected in Table 2. Table 1 shows that the Si–30Zr catalyst is more selective to acrolein within the first 5 h of reaction, but acrolein was not detected among the products after 24 h of TOS, whereas the hydroxyacetone selectivity increased up to 46 mol%. Moreover, Si–30Zr is less resistant to the deactivation since glycerol conversion drops up to 12 mol% after 24 h of TOS. Therefore, the incorporation of zirconium into the siliceous network gives rise to acid catalysts with a catalytic performance in the glycerol dehydration better than that exhibited when ZrO_2 is dispersed on the mesoporous silica walls.

3.3. Coke characterization

Taking into account that catalyst deactivation is an important drawback for most of catalysts in the glycerol dehydration, spent catalysts have been characterized after the catalytic test in order to know the nature of the adsorbed species, which could be responsible of deactivation. Prior to the characterization, these spent catalysts have been dried in situ under the carrier gas stream. A considerable amount of carbonaceous deposits could be inferred from the dark colour of the spent catalysts. The results of their textural characterization (Table 5) reveal a noticeable decrease in the S_{BET} and pore volume values, which is more important for the SiZr10 catalyst. This catalyst showed the lowest values of pore diameter and pore volume among the tested catalysts, which could be explained by the presence of carbonaceous deposits blocking the porous network. Thus, it is observed that the more acidic catalyst displays the highest weight loss, as measured by TG analysis, after the catalytic run (Table 5). The H/C ratios of the carbonaceous deposits formed at 325 °C suggest that the deposits are hydrogen deficient, which can be associated to species highly condensed like aromatic molecules. The formation of these molecules could be due to consecutive reactions of glycerol, as well as to side reactions between products [16].

The thermal stability of carbonaceous deposits has been studied by means of DTA and EGA-MS analysis. The DTA curves of the spent catalysts (Fig. 7) show two overlapped exothermic peaks extending from 150 to 700 °C. The shape of these curves point out the presence of different types of carbonaceous deposits on the surface of the catalysts The first peak is more intense for all catalysts and the maxima are observed at 363 and 383 °C for SiZr5 and SiZr10 catalysts, respectively. This first peak could be ascribed to carbon deposits easily oxidized [9] like aliphatic molecules [26]. Meanwhile, the second peak is discernible for the SiZr4 and SiZr10 catalysts but it appears like a shoulder and at lower temperature for the SiZr5 catalyst. This peak at higher temperature could be ascribed to carbon deposits more difficult to burn, such as those associated to polyaromatic molecules [26]. Among the tested catalysts, the SiZr4 catalyst shows a larger quantity of heat emitted during the burning of the carbonaceous deposits, pointing out a higher amount of

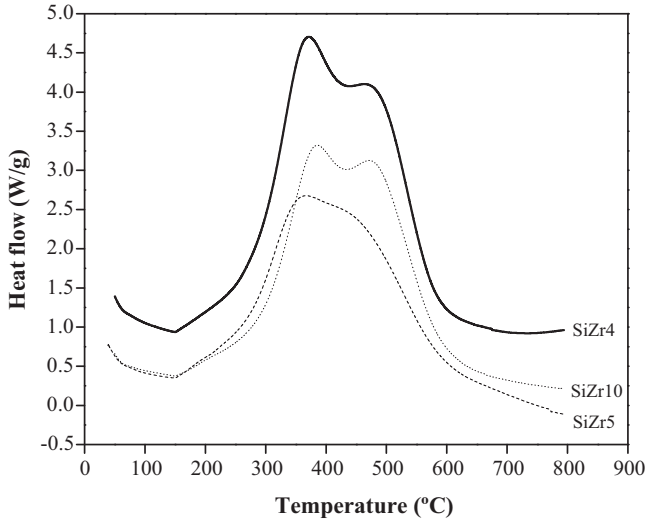

Fig. 7. DTA analysis of spent catalysts.

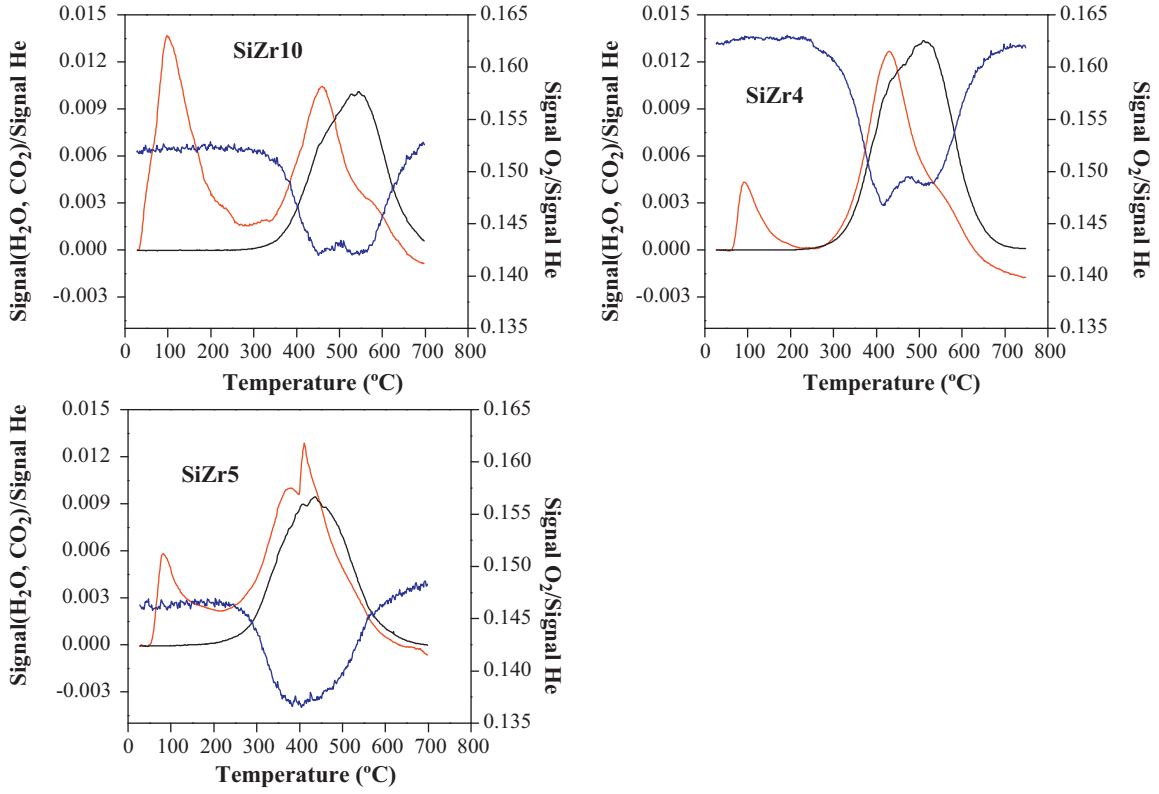

Fig. 8. EGA-MS analysis of the spent catalysts. Red line: evolved water; Black line: evolved carbon dioxide and blue line: evolved oxygen.

carbonaceous deposits on the surface of this catalyst such as TG analysis shown.

The EGA-MS analysis has been also used to study the carbonaceous deposits in the spent catalysts. The catalysts have been heated in a flow of oxygen (5 vol.% in He) from 25 °C to 800 °C. Fig. 8 displays the consumption of O_2 as well as the evolved CO_2 and H_2O during the combustion of carbonaceous deposits formed during the catalytic tests at 325 °C over the SiZr5 catalyst. The evolved H_2O curve shows a peak at low temperature without emission of CO_2, which can be ascribed to the physisorbed water not evacuated on the catalyst surface after the drying treatment. Between 200 and 700 °C, the H_2O curve shows two peaks at 376 and 411 °C and a shoulder at 520 °C. These peaks are associated to the combustion of carbonaceous deposits since the evolved H_2O is accompanied by the releasing of CO_2. The curve of evolved CO_2 emission is fairly symmetrical in the temperature range from 200 to 700 °C; this fact along with the intensity of CO_2 and H_2O signals could indicate the presence of highly hydrogenated carbonaceous species, which would be of aliphatic nature. This is consistent with the results of DTA analysis, which showed that the deposits on this catalyst were less resistant to combustion. However, the composition of the coke deposited on SiZr10 and SiZr4 catalysts may differ from the SiZr5. On one hand, the curve of evolved H_2O also shows a peak at temperatures lower than 100 °C due to physisorbed H_2O and a band extending from 250 to 700 °C with a maximum at 430 °C and a shoulder at 560 °C. The peak at 430 °C is accompanied by the emission of CO_2 with a similar intensity. This peak, as in the case of the SiZr5 catalyst, is due to aliphatic carbon species, while the shoulder at 560 °C is accompanied by a more intense emission of CO_2, indicating that these species are more deficient in hydrogen, perhaps unsaturated hydrocarbon more resistant to combustion. In conclusion, the DTA and EGA-MS analysis shows that the coke deposited on the SiZr5 catalyst is more aliphatic than deposited in the other two catalysts which present more unsaturated species.

4. Conclusions

A series of zirconium doped mesoporous silica, with different Si/Zr molar ratios, has been synthesized and tested in the gas-phase dehydration of glycerol. NH_3-TPD and pyridine adsorption coupled to FTIR spectroscopy has revealed the presence of well dispersed acid sites, mainly of Lewis type, associated to Zr(IV) species deficiently coordinated located on the pore walls of the siliceous framework. The glycerol conversion increases with the zirconium content, reaching values higher than 90 mol% for a Si/Zr molar ratio of 4, at 325 °C after 5 h of TOS. However, the catalysts suffer from deactivation, which is more important when zirconium oxide is incorporated by impregnation of a mesoporous MCM-41 silica. EGA-MS and TG-DTA have demonstrated that the carbonaceous deposits are mainly aliphatic molecules, except for the SiZr5 catalysts, where the presence of saturated species is detected. The acrolein yield is in all cases lower than 23 mol%, but the pretreatment under a saturated-steam helium flow allows reaching an acrolein yield of 38 mol% and ameliorates the stability of catalysts. The selectivity towards acrolein and hydroxyacetone can be explained by considering the influence of the nature of active sites.

Acknowledgments

The authors are grateful to the Spanish Ministry of Science and Innovation (ENE2009-12743-C04-03 project), Junta de Andalucía (P09-FQM-5070) and FEDER funds for financial support. RMT would like to thank the Ministry of Science and Innovation for the financial support under the Program Ramón y Cajal (RYC-2008-03387).

References

[1] Y. Moro-Oka, W. Ueda, Adv. Catal. 40 (1994) 233–273.
[2] C. Huang, W. Guo, X. Yi, W. Weng, H. Wan, Catal. Commun. 8 (2007) 162–166.

[3] F. Ivars, B. Solsona, S. Hernández, J.M. López Nieto, Catal. Today 149 (2010) 260–266.
[4] B. Katryniok, S. Paul, V. Bellière-Baca, P. Rey, F. Dumeignil, Green Chem. 12 (2010) 2079–2098.
[5] P. Sabatier, G. Gaudion, Compt. Rend. 166 (1918) 1033–1039.
[6] C.J. Zhou, C.J. Huang, W.G. Zhang, H.S. Zhai, H.L. Wu, Z.S. Chao, Stud. Surf. Sci. Catal. 165 (2007) 527–530.
[7] E. Yoda, A. Ootawa, Appl. Catal. A 360 (2009) 66–70.
[8] Y.T. Kim, K.D. Jung, E.D. Park, Microporous Mesoporous Mater. 131 (2010) 28–36.
[9] C.J. Jia, Y. Liu, W. Schmidt, A.H. Lu, F. Schüth, J. Catal. 269 (2010) 71–79.
[10] A.S. de Oliveira, S.J.S. Vasconcelos, J.R. de Sousa, F.F. de Sousa, J.M. Filho, A.C. Oliveira, Chem. Eng. J. 168 (2011) 765–774.
[11] S.H. Chai, H.P. Wang, Y. Liang, B.-Q. Xu, Appl. Catal. A 353 (2009) 213–222.
[12] S.H. Chai, H.P. Wang, Y. Liang, B.Q. Xu, Green Chem. 10 (2008) 1087–1093.
[13] E. Tsukuda, S. Sato, R. Takahashi, T. Sodesawa, Catal. Commun. 8 (2007) 1349–1353.
[14] H. Atia, U. Armbruster, A. Martin, J. Catal. 258 (2008) 71–82.
[15] W. Yan, G.J. Suppes, Ind. Eng. Chem. Res. 48 (2009) 3279–3283.
[16] W. Suprun, M. Lutecki, T. Haber, H. Papp, J. Mol. Catal. A 309 (2009) 71–78.
[17] S.H. Chai, H.P. Wang, Y. Liang, B.Q. Xu, J. Catal. 250 (2007) 342–349.
[18] N.R. Shiju, D.R. Brown, K. Wilson, G. Rothenberg, Top. Catal. 53 (2010) 1217–1223.
[19] A. Ulgen, W. Hoelderich, Catal. Lett. 131 (2009) 122–128.
[20] A. Ulgen, W.F. Hoelderich, Appl. Catal A 400 (2011) 34–38.
[21] K. Pathak, K.M. Reddy, N.N. Bakhshi, A.K. Dalai, Appl. Catal. A 372 (2010) 224–238.
[22] H. Atia, U. Armbruster, A. Martin, Appl. Catal. A 393 (2011) 331–339.
[23] C.L. Lima, S.J.S. Vasconcelos, J.M. Filho, B.C. Neto, M.G.C. Rocha, P. Bargiela, A.C. Oliveira, Appl. Catal. A 399 (2011) 50–62.
[24] D. Stosic, S. Bennici, J-L. Couturier, J.-L. Dubois, A. Auroux, Catal. Commun. 17 (2012) 23–28.
[25] A. Corma, G.W. Huber, L. Sauvanaud, P. O'Connor, J. Catal. 257 (2008) 163–171.
[26] A. Alhanash, E.F. Kozhevnikova, I.V. Kozhevnikov, Appl. Catal. A 378 (2010) 11–18.
[27] P. Lauriol-Garbay, J.M.M. Millet, S. Loridant, V. Bellière-Baca, P. Rey, J. Catal. 280 (2011) 68–76.
[28] D.J. Jones, J. Jiménez-Jiménez, A. Jiménez-López, P. Maireles-Torres, P. Olivera-Pastor, E. Rodríguez-Castellón, J. Rozière, Chem. Commun. 5 (1997) 431–432.
[29] E. Rodríguez-Castellón, A. Jiménez-López, P. Maireles-Torres, D.J. Jones, J. Rozière, M. Trombetta, G. Busca, M. Lenarda, L. Storaro, J. Solid State Chem. 175 (2003) 159–169.
[30] A. Jiménez-López, E. Rodríguez-Castellón, P. Maireles-Torres, L. Díaz, J. Mérida-Robles, Appl. Catal. A 218 (2001) 295–306.
[31] M.C. Carrión, B.R. Manzano, F.A. Jalón, D. Eliche-Quesada, P. Maireles-Torres, E. Rodríguez-Castellón, A. Jiménez-López, Green Chem. 7 (2005) 793–799.
[32] S.H. Chai, H.P. Wang, Y. Liang, B.Q. Xu, Green Chem. 9 (2007) 1130–1136.
[33] Q. Liu, Z. Zhang, Y. Du, J. Li, X. Yang, Catal. Lett. 127 (2009) 419–428.
[34] Y.T. Kim, K.-D. Jung, E.D. Park, Appl. Catal. A 393 (2011) 275–287.
[35] P. Berteau, B. Delmon, Catal. Today 5 (1989) 121–137.
[36] C. García-Sancho, R. Moreno-Tost, J.M. Mérida-Robles, J. Santamaría-González, A. Jiménez-López, P. Maireles-Torres, Appl. Catal. B 108–109 (2011) 161–167.
[37] W. Suprun, M. Lutecki, R. Gläser, H. Papp, J. Mol. Catal. A 342–343 (2011) 91–100.
[38] A. Ramanathan, M.C. Castro Villalobos, S. Cees Kwakernaak, U. Telalovic, Hanefeld, Chem. Eng. J. 14 (2008) 961–972.
[39] M. Knapczyk, M. Motek, W. Suprun, H. Papp, T. Grybeck, Catal. Today 176 (2011) 331–335.
[40] Q. Zhao, X. Zhou, Y. Li, T. Jiang, H. Yin, C. Li, Appl. Surf. Sci. 255 (2009) 6397–6403.
[41] T.S. Jiang, X.P. Zhou, Y.H. Li, Q. Zhao, H.B. Yin, Inorg. Mater. 47 (2011) 296–302.
[42] G. Busca, Catal. Today 41 (1998) 191–206.
[43] F. Cavani, S. Guidetti, L. Martinelli, M. Piccinini, E. Ghedini, M. Signoretto, Appl. Catal. B 100 (2011) 197–204.
[44] D. Carriazo, C. Domingo, C. Martin, V. Rives, J. Solid State Chem. 181 (2008) 2046–2057.
[45] P. Salas, J.A. Wang, H. Armendariz, C. Angeles-Chavez, L.F. Chen, Mater. Chem. Phys. 114 (2009) 139–144.
[46] J.M.R. Gallo, C. Bisio, G. Gatti, L. Marchese, H.O. Pastore, Langmuir 26 (2010) 5791–5800.
[47] J.A. Anderson, C. Fergusson, I. Rodríguez-Ramos, A. Guerrero-Ruiz, J. Catal. 192 (2000) 344–354.
[48] M.D. Gracia, A.M. Balu, J.M. Campelo, R. Luque, J.M. Marinas, A.A. Romero, Appl. Catal. A 37 (2009) 85–91.
[49] J. Iglesias, J.M. Melero, L.F. Bautista, G. Morales, R. Sánchez-Vázquez, M.Y. Andreola, A. Lizarraga-Fernández, Catal. Today 167 (2011) 46–55.
[50] P. Lauriol-Garbey, S. Loridant, V. Bellière-Baca, P. Rey, J.M.M. Millet, Catal. Commun. 16 (2011) 170–174.
[51] F. Wang, J.L. Dubois, W. Ueda, J. Catal. 268 (2009) 260–267.
[52] L.-Z. Tao, S.-H. Chai, Y. Zuo, W.T. Zheng, Y. Liang, B-Q. Xu, Catal. Today 158 (2010) 310–316.
[53] M.H. Haider, N.F. Dummer, D. Zhang, P. Miedziak, T.E. Davies, S.H. Taylor, D.J. Willock, D.W. Knight, D. Cadwick, G.J. Hutchings, J. Catal. 286 (2012) 206–213.
[54] Y.T. Kim, K.D. Jung, E.D. Park, Bull. Korean Chem. Soc. 11 (2010) 3283–3290.
[55] Y.T. Kim, K.D. Jung, E.D. Park, Appl. Catal. B 107 (2011) 177–187.
[56] F. Auneau, C. Michel, F. Delbecq, C. Pinel, P. Sautet, Chem. Eur. J. 17 (2011) 14288–14299.